Loss-of-function mutations in *ADCY3* cause monogenic severe obesity

Sadia Saeed [1,2], Amélie Bonnefond[1], Filippo Tamanini[2], Muhammad Usman Mirza [3], Jaida Manzoor[4], Qasim M. Janjua [5], Sadia M. Din[6], Julien Gaitan[7,8], Alexandra Milochau[7,8], Emmanuelle Durand[1], Emmanuel Vaillant[1], Attiya Haseeb[6], Franck De Graeve[1], Iandry Rabearivelo[1], Olivier Sand[1], Gurvan Queniat[1], Raphaël Boutry[1], Dina A. Schott[9], Hina Ayesha[10], Muhammad Ali[11], Waqas I. Khan[12], Taeed A. Butt[13], Tuula Rinne [14], Connie Stumpel[15], Amar Abderrahmani[1,2], Jochen Lang [7,8], Muhammad Arslan[5,6] and Philippe Froguel [1,2]*

Study of monogenic forms of obesity has demonstrated the pivotal role of the central leptin–melanocortin pathway in controlling energy balance, appetite and body weight[1]. The majority of loss-of-function mutations (mostly recessive or co-dominant) have been identified in genes that are directly involved in leptin–melanocortin signaling. These genes, however, only explain obesity in <5% of cases, predominantly from outbred populations[2]. We previously showed that, in a consanguineous population in Pakistan, recessive mutations in known obesity-related genes explain ~30% of cases with severe obesity[3–5]. These data suggested that new monogenic forms of obesity could also be identified in this population. Here we identify and functionally characterize homozygous mutations in the *ADCY3* gene encoding adenylate cyclase 3 in children with severe obesity from consanguineous Pakistani families, as well as compound heterozygous mutations in a severely obese child of European-American descent. These findings highlight ADCY3 as an important mediator of energy homeostasis and an attractive pharmacological target in the treatment of obesity.

Obesity, with its complications, has emerged as a major contributor to the global health burden and has assumed the status of a pandemic[6]. At least 2.8 million people die each year as a consequence of being overweight or obese[7]. Although obesity is one of the most heritable diseases[8], the genetic etiology of a large proportion of obesity cases remains elusive.

Here we performed whole-exome sequencing (WES) analysis in 138 probands who presented with severe, early-onset obesity (body mass index (BMI) s.d. score (SDS) ≥3) and their available family members (*n* = 117) from consanguineous families from the Punjab province of Pakistan. These 138 probands were part of a larger cohort of 195 probands, 57 of whom were previously found to carry mutations in known obesity-related genes and were excluded from the present investigation (published[3–5] and unpublished data; Fig. 1a). Through successive filtration steps (Fig. 1a), we identified four severely obese children from three unrelated families (Fig. 1b, families (F) 1–3) who had new or extremely rare homozygous mutations in *ADCY3*. The three potentially causative mutations included a frameshift mutation, c.3315del (NM_004036.4), which encodes p.Ile1106Serfs*3 (NP_004027.2) (hereafter referred to as *ADCY3*[Mut-I]); a splice-site mutation, c.2578−1G>A (hereafter referred to as *ADCY3*[Mut-II]); and a nonsynonymous missense mutation, c.191A>T, which encodes p.Asn64Ile (hereafter referred to as *ADCY3*[Mut-III]) (Fig. 1b,c and Supplementary Fig. 1). Both the *ADCY3*[Mut-I] and *ADCY3*[Mut-II] variants were new and not present in the Exome Aggregation Consortium (ExAC) dataset, dbSNP or the Exome Sequencing Project (ESP) database. The splice-site variant *ADCY3*[Mut-II] was predicted to abolish the splice acceptor site (Supplementary Note). *ADCY3*[Mut-III] (rs541941351) is documented in the ExAC database with a global frequency of 3×10^{-4}. All of the parents were heterozygous carriers of the respective *ADCY3* mutations (Fig. 1b and Supplementary Table 1). *ADCY3* was found within a large (30- to 68-Mb) region of homozygosity that was shared by affected subjects (data not shown). Notably, our filtration process did not report recessive variants in any other gene that putatively causes monogenic obesity (Fig. 1a and Supplementary Tables 2–4).

In a separate and independent investigation, WES analysis identified a compound heterozygous *ADCY3* mutation in a child with severe obesity who was from a nonconsanguineous family of European-American heritage (Fig. 1b, F-4). This compound heterozygous mutation included a frameshift mutation, c.1268del (which encodes p.Gly423Alafs*19; hereafter referred to as *ADCY3*[Mut-IVa]) and one that resulted in an amino acid deletion, c.3354_3356del (which encodes p.Phe1118del; hereafter referred to as *ADCY3*[Mut-IVb])
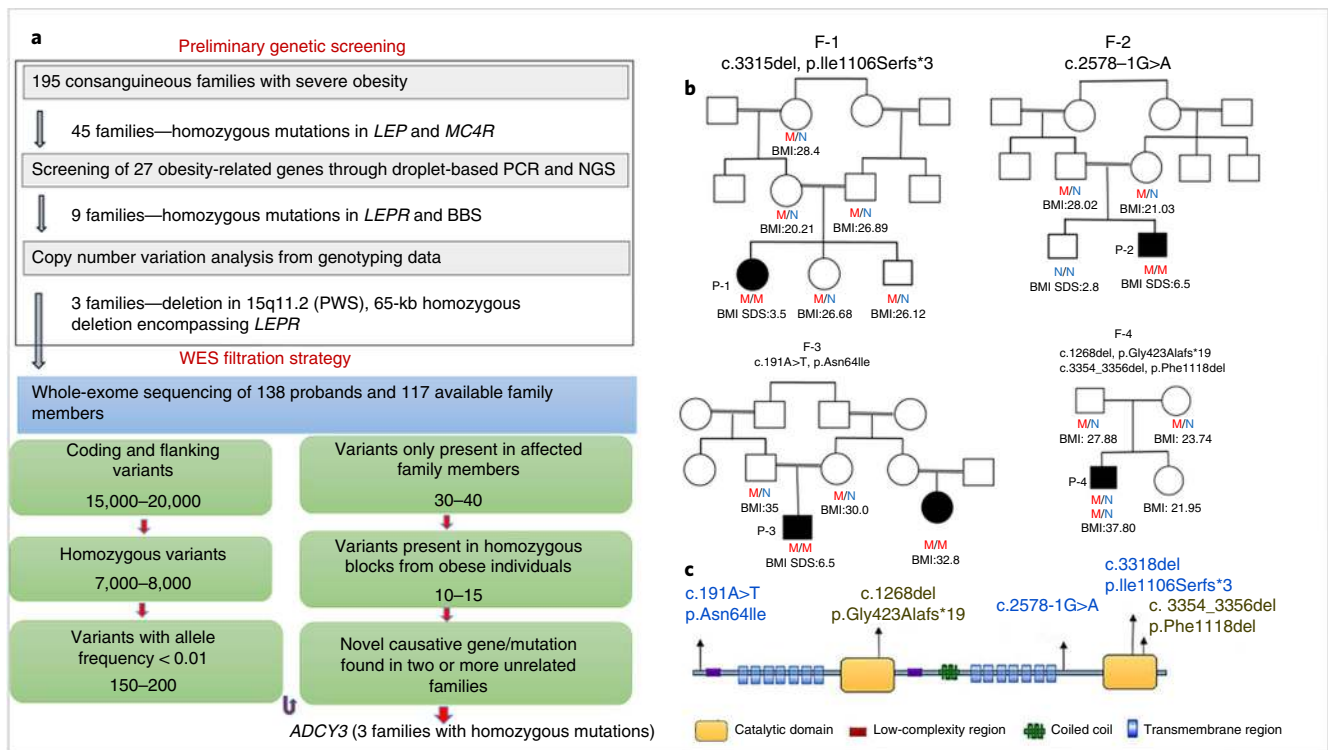
Fig. 1 | *ADCY3* mutations identified in four affected families. a, Schematic of the stepwise genetic screening of 195 probands affected with severe obesity from a consanguineous population from Pakistan; 57 probands carried mutations in known obesity-related genes and were excluded from further analyses. WES analysis was performed in the remaining 138 probands and 117 family members. **b**, Pedigrees of four affected families (F-1 to F-4) showing mutation status (N, normal allele; M, mutant allele), BMI value and the BMI SDS. P, proband. **c**, Position of mutations identified in *ADCY3* in relation to the encoded ADCY3 domains (NM_004036.4).

(Fig. 1c and Supplementary Fig. 1). The *ADCY3*^Mut-IVa^ variant was new, whereas the *ADCY3*^Mut-IVb^ (rs750852737) variant has been documented in the ExAC dataset with a global frequency of 4×10^{-5}. *ADCY3*^Mut-IVa^ and *ADCY3*^Mut-IVb^ were paternally and maternally inherited, respectively (Supplementary Fig. 1). All of the observed mutated sites in *ADCY3* are highly conserved across various species, suggesting that these sites have evolutionary significance (Supplementary Fig. 2).

ADCY3 is a member of a family of ten related cyclases that catalyze the synthesis of cyclic AMP (cAMP) from ATP, of which nine are anchored to the plasma membrane. We first assessed the dynamic and structural consequences of the mutations on ATP binding. Homology modeling followed by molecular dynamics (MD) simulations was performed to investigate conformational changes in terms of the root-mean-square deviation (r.m.s. deviation) parameter (Fig. 2a–c and Supplementary Note). Structural analysis was possible for only the ADCY3^Mut-I^ and ADCY3^Mut-II^ proteins, for which the crystal structures of the relevant ADCY3 domains were available. The structures of the mutant proteins showed destabilization of the backbone atoms, which resulted in partial unfolding of the catalytic domains. These changes in the mutant proteins displaced ATP from its binding site, whereas the wild-type (WT) protein remained stable for the entire simulation period. The residual flexibility profile for each of the two proteins indicated more fluctuations (r.m.s. fluctuation; RMSF) in the mutant proteins than in WT ADCY3, thus predicting the inability of the mutant protein to bind ATP. We therefore hypothesized that these mutations would result in destabilization of the ADCY3 catalytic domains, leading to a loss of protein function.

To further test this hypothesis, we transiently overexpressed recombinant Myc-tagged WT ADCY3 (Myc-hADCY3^WT^) or each of the four mutant proteins (Myc-ADCY3^Mut-I^, Myc-ADCY3^Mut-II^, Myc-ADCY3^Mut-III^ and Myc-ADCY3^Mut-IVb^) in baby hamster kidney (BHK) cells. The expression and cellular localization of the Myc-tagged WT and mutant ADCY3 proteins were equivalent, as monitored by protein blotting and immunofluorescence analyses (Supplementary Figs. 3 and 4). Also, transient expression of either Myc-hADCY3^WT^ or each of the mutant variants did not significantly alter basal cAMP levels as compared to those in cells transfected with the control plasmid (Fig. 2d). Stimulation of adenylate cyclase activity by treatment of the cells with forskolin and concomitant inhibition of endogenous phosphodiesterases by treatment with 3-isobutyl-1-methylxanthine (IBMX) led to a significantly greater increase in cAMP levels in cells that overexpressed either Myc-hADCY3^WT^ or Myc-ADCY3^Mut-III^ (~50-fold relative to nontreated cells) versus those that expressed the control plasmid, Myc-ADCY3^Mut-I^, Myc-ADCY3^Mut-II^ or Myc-ADCY3^Mut-IVb^ (~25-fold increase relative to untreated cells) (Fig. 2d). These data provide support for the idea that catalytic activity is affected in ADCY3^Mut-I^, ADCY3^Mut-II^ and ADCY3^Mut-IVb^ but not in ADCY3^Mut-III^. Similar results were found by using luciferase assays—the stimulatory effect of ADCY3^Mut-I^, ADCY3^Mut-II^ and ADCY3^Mut-IVb^ on the activity of a cAMP-responsive element reporter construct (CRE-Luc) in response to IBMX and forskolin treatment was lower (9-fold, 7-fold and 9-fold increase, respectively) than that for hADCY3^WT^ (13-fold increase) and ADCY3^Mut-III^ (11-fold increase) (Supplementary Fig. 5). Characterization of the protein encoded by a nonsynonymous (p.Ser107Pro) and common SNP variant (rs11676272) in identical assays showed catalytic activity comparable to that of hADCY3^WT^ (Supplementary Fig. 6). Notably, evaluation of *ADCY3* mRNA levels in the white blood cells of the members of family 1 (F-1; for whom mRNA was available) showed that these were similar in the affected child carrying a homozygous
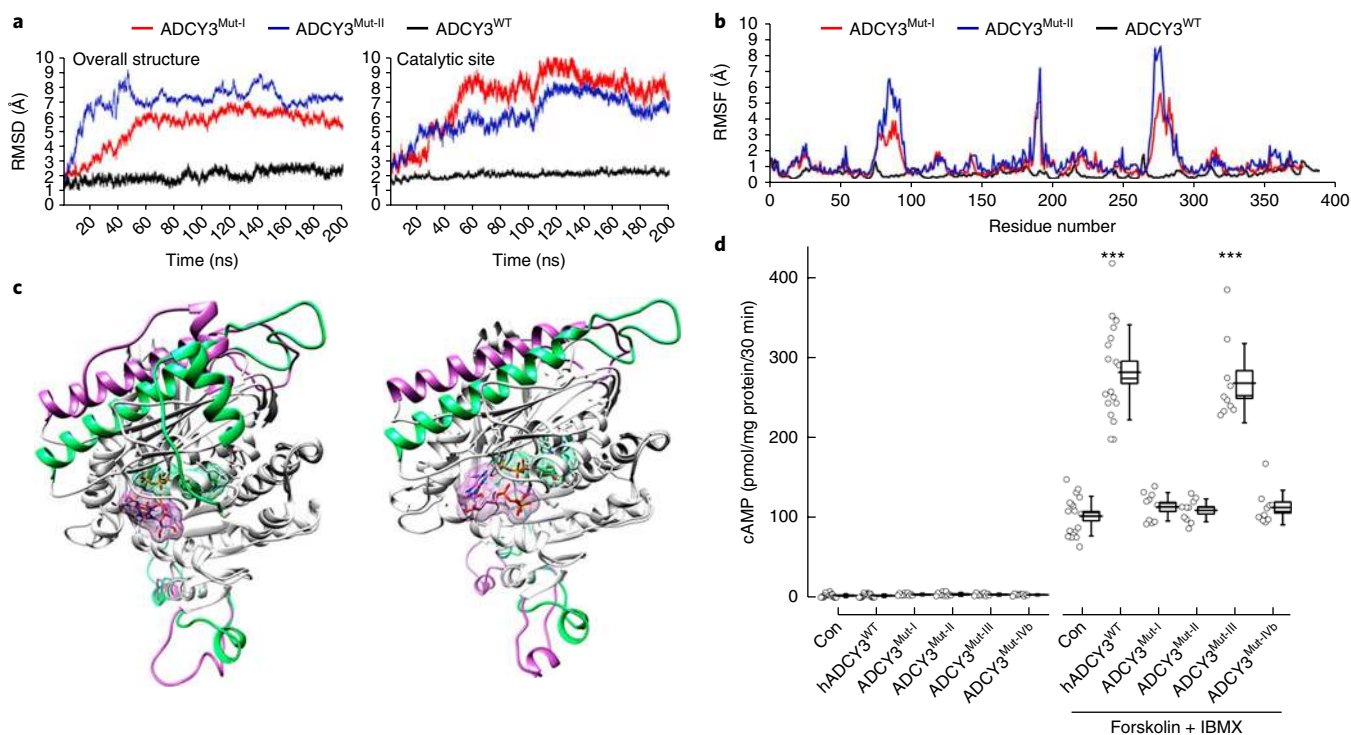
Fig. 2 | Effect of wild-type and mutant ADCY3. a, Representative curve of backbone stability of the whole protein (left) and of the catalytic site (right), as assessed during a 200-ns MD simulation in terms of r.m.s. deviation (RMSD), for hADCY3[WT] (black), ADCY3[Mut-I] (red) and ADCY3[Mut-II] (blue). The mutants showed high conformational fluctuations, particularly at the catalytic site. **b**, Residual flexibility profile for hADCY3[WT] (black), ADCY3[Mut-I] (red) and ADCY3[Mut-II] (blue) during a 200-ns MD simulation, as calculated by r.m.s. fluctuation (RMSF), presented higher fluctuations in the ADCY3 mutants than in WT ADCY3. **c**, Superimposed structures of ADCY3[Mut-I] (left) and ADCY3[Mut-II] (right) before (green) and after (purple) 200-ns MD simulations. The docked conformations, in which an ATP molecule interacts with the catalytic region, are displayed with initial and simulated conformations in the green and purple mesh-surface representation, respectively. The gray regions indicate the least fluctuated segments of the proteins. **d**, cAMP production in the absence or presence of forskolin and IBMX treatment (30 min) in BHK cells that had been transfected with control plasmid (pcDNA3) or with plasmid encoding hADCY3[WT], ADCY3[Mut-I], ADCY3[Mut-II], ADCY3[Mut-III] or ADCY3[Mut-IVb] ($n = 18$ independent experiments for control and hADCY3[WT]; $n = 10$ independent experiments for ADCY3[Mut-I], ADCY3[Mut-II], ADCY3[Mut-III] and ADCY3[Mut-IVb]). Data are presented in box-and-whisker plots (box represents 2nd and 3rd quartiles and whiskers indicate 1st and 4th quartiles). Individual data are presented by circles. ***$P < 0.001$ by ANOVA followed by Bonferroni *post hoc* test.

ADCY3[Mut-I] mutation and her unaffected heterozygous sibling (Supplementary Fig. 7).

Taken together, these data imply that *ADCY3*[Mut-I], *ADCY3*[Mut-II] and *ADCY3*[Mut-IVb] are loss-of-function variants that dramatically and directly affect the catalytic activity of the encoded protein and, thereby, cAMP production. *ADCY3*[Mut-III], which failed to alter ADCY3 catalytic activity, encodes a small polar amino acid residue (replacing a large hydrophobic residue) in the globular cytosolic N-terminal domain that likely restricts the protein conformation. This suggests that *ADCY3*[Mut-III] might lead to impaired ADCY3 function and thereby promote obesity in the affected patient via impaired G-protein-coupled receptor interactions. However, the possibility remains that there is another obesity-associated mutation in this proband that was missed by our very stringent gene-screening strategy. Overall, our genetic and functional data support the identification of a novel form of monogenic obesity associated with mutations in *ADCY3*.

Consistent with our observations of subjects with *ADCY3* mutations (Fig. 1 and Table 1), *Adcy3*^{−/−} mice are hyperphagic and obese[9]. Hyperphagia in the probands was first reported between 0.5 and 2.0 years of age. Family members who were WT or heterozygous for *ADCY3* presented normal body weight, except for the parents of proband 2 (P2), who reportedly were accustomed to fat- and carbohydrate-enriched food (Supplementary Table 1). Notably, the three probands P1, P3 and P4 were anosmatic when clinically tested, an observation that is in agreement with findings in *Adcy3*^{−/−} mice[10].

Sense of smell was, however, only slightly abnormal in P2 and his affected cousin. Two affected patients (P1 and P3) had slight-to-moderate intellectual disability despite normal body growth, whereas probands P2 and P4 did not have any intellectual disabilities. No dysmorphic features were observed. The only affected female (P1), the oldest of the four probands, experienced menarche at 14 years of age but had no subsequent menstrual cycles. In this subject, excessive adiposity was accompanied by hyperlipidemia and insulin resistance (Table 1 and Supplementary Tables 5 and 6). These observations are also consistent with those of *Adcy3*^{−/−} mice, which exhibit an age-related increase in adiposity[9].

ADCY3 is expressed in the hypothalamus, and selective ablation of *Adcy3* in the mouse hypothalamus results in a significant increase in body fat mass[11]. Conversely, mice with a gain-of-function mutation in *Adcy3* have less fat than WT mice and are resistant to obesity when fed a high-fat diet[12]. ADCY3 is known to mediate the action of hormones involved in energy, lipid and glucose control[13]. Anorexigenic gut peptides, such as GLP1, that utilize G-protein-coupled receptors for signaling act centrally to control appetite by upregulating ADCY3-mediated cAMP production[14]. Moreover, the antidiabetic drug liraglutide (a GLP1 agonist) enhances expression of *Adcy3* at the mRNA and protein levels[15], resulting in a weight-reducing effect through its direct effect on the hypothalamus[16]. This suggests that pathogenic mutations in *ADCY3* result in interference of several anorexigenic signaling cascades. Furthermore, ADCY3–cAMP signaling is also known to regulate the proliferation

Table 1 | Physical and endocrine characteristics for the four probands (P1 to P4) with mutations in the _ADCY3_ gene

Characteristic	P1	P2	P3	P4
	_ADCY3_Mut-I	_ADCY3_Mut-II	_ADCY3_Mut-III	_ADCY3_Mut-IVa/Mut-IVb
Physical				
Sex	Female	Male	Male	Male
Age (years)	15	6	6	11
Height (cm)	150	137	132	154
Body weight (kg)	87	52	49	89
BMI	38.7	28.0	28.1	37.8
BMI SDS for age	3.5	6.5	6.5	4.6
Endocrine				
Insulin (μU/ml)	48	11	13	–
Leptin (ng/ml)	30	22	11	–
Cortisol (μg/dl)	18	11	7.5	–

_ADCY3_Mut-I, homozygous frameshift mutation (p.Ile1106Serfs*3); _ADCY3_Mut-II, homozygous splice-site mutation (c.2578−1G>A); _ADCY3_Mut-III, homozygous missense mutation (p.Asn64Ile); _ADCY3_Mut-IVa/Mut-IVb, compound heterozygous mutation ([p.Phe1118del] + [p.Gly423Alafs*19]). Reference values (mean ± s.e.m.) from age-matched subjects with severe obesity of unknown genetic causality from the same population: BMI, 33.8 ± 1.1 (_n_ = 46); BMI SDS for age, 5.1 ± 0.3 (_n_ = 46); insulin, 35 ± 2.6 μU/ml (_n_ = 32); leptin, 30 ± 1.5 ng/ml (_n_ = 32); cortisol (morning sample), 20 ± 0.4 μg/dl (_n_ = 32). Reference values (mean ± s.e.m.) from age-matched subjects with WT _ADCY3_ from the same population (_n_ = 33): BMI, 17.0 ± 1.0; BMI SDS for age, −0.4 ± 0.1; insulin, 7 ± 1.0 μU/ml; leptin, 3 ± 0.4 ng/ml; cortisol, 1 ± 0.4 μg/dl.

and differentiation of adipocytes and intracellular processes related to adipogenesis and lipolysis[17]. _Adcy3_ haploinsufficient (_Adcy3+/−_) mice exhibit increased adipogenesis and adiposity without hyperphagia[18]. Therefore, potent peripheral ADCY3–cAMP-driven regulation of adiposity and body weight may also exist in humans, and pharmacological compounds that affect ADCY3 activity may elicit beneficial effects in obese individuals.

Our genetic and functional human data strongly suggest that recessive pathogenic mutations in _ADCY3_ cause monogenic severe obesity. Of note, genome-wide association studies (GWAS) have demonstrated a consistent association between frequent variants in _ADCY3_ and both BMI and fat mass[19–24], which is reminiscent of _MC4R_ and _PCSK1_, for which both frequent and rare DNA variants have also been linked to common and monogenic obesity, respectively[21]. Apart from its association with obesity-related traits, ADCY3 has been implicated through GWAS in other disorders including ulcerative colitis, inflammatory bowel disease and Crohn's disease[25]. Furthermore, increased methylation of sites in _ADCY3_ and its promoter region has been associated with increased BMI[26,27]. _ADCY3_-associated obesity, therefore, recapitulates both the genetic and epigenetic mechanisms that have previously been shown for _POMC_[26]. Identification of novel forms of monogenic obesity in consanguineous families makes it important to screen inbred populations in the quest to identify novel pathways and physiological mechanisms leading to obesity that could remain unexposed in nonconsanguineous populations.

Methods

Methods, including statements of data availability and any associated accession codes and references, are available at https://doi.org/10.1038/s41588-017-0023-6.

References

1. El-Sayed Moustafa, J. S. & Froguel, P. From obesity genetics to the future of personalized obesity therapy. _Nat. Rev. Endocrinol._ **9**, 402–413 (2013).
2. Froguel, P. & Blakemore, A. I. The power of the extreme in elucidating obesity. _N. Engl. J. Med._ **359**, 891–893 (2008).
3. Saeed, S. et al. Novel _LEPR_ mutations in obese Pakistani children identified by PCR-based enrichment and next-generation sequencing. _Obesity (Silver Spring)_ **22**, 1112–1117 (2014).
4. Saeed, S. et al. Genetic variants in _LEP_, _LEPR_ and _MC4R_ explain 30% of severeobesity in children from a consanguineous population. _Obesity (Silver Spring)_ **23**, 1687–1695 (2015).
5. Saeed, S., Butt, T. A., Anwer, M., Arslan, M. & Froguel, P. High prevalence of leptin and melanocortin-4 receptor gene mutations in children with severe obesity from Pakistani consanguineous families. _Mol. Genet. Metab._ **106**, 121–126 (2012).
6. Kopelman, P. G. Obesity as a medical problem. _Nature_ **404**, 635–643 (2000).
7. World Health Organization. _A Snapshot of Global Health_ (World Health Organization, Geneva, 2012).
8. Stunkard, A. J., Harris, J. R., Pedersen, N. L. & McClearn, G. E. The body mass index of twins who have been reared apart. _N. Engl. J. Med._ **322**, 1483–1487 (1990).
9. Wang, Z. et al. Adult type 3 adenylyl-cyclase-deficient mice are obese. _PLoS One_ **4**, e6979 (2009).
10. Wong, S. T. et al. Disruption of the type III adenylyl cyclase gene leads to peripheral and behavioral anosmia in transgenic mice. _Neuron_ **27**, 487–497 (2000).
11. Cao, H., Chen, X., Yang, Y. & Storm, D. R. Disruption of type 3 adenylyl cyclase expression in the hypothalamus leads to obesity. _Integr Obes Diabetes_ **2**, 225–228 (2016).
12. Pitman, J. L. et al. A gain-of-function mutation in adenylate cyclase 3 protects mice from diet-induced obesity. _PLoS One_ **9**, e110226 (2014).
13. Hanoune, J. & Defer, N. Regulation and role of adenylyl cyclase isoforms. _Annu. Rev. Pharmacol. Toxicol._ **41**, 145–174 (2001).
14. Kanoski, S. E., Fortin, S. M., Arnold, M., Grill, H. J. & Hayes, M. R. Peripheral and central GLP1 receptor populations mediate the anorectic effects of peripherally administered GLP1 receptor agonists, liraglutide and exendin-4. _Endocrinology_ **152**, 3103–3112 (2011).
15. Liang, Y. et al. Hepatic adenylate cyclase 3 is upregulated by liraglutide and subsequently plays a protective role in insulin resistance and obesity. _Nutr. Diabetes_ **6**, e191 (2016).
16. Ando, T. et al. Liraglutide as a potentially useful agent for regulating appetite in diabetic patients with hypothalamic hyperphagia and obesity. _Intern. Med._ **53**, 1791–1795 (2014).
17. Madsen, L. & Kristiansen, K. The importance of dietary modulation of cAMP and insulin signaling in adipose tissue and the development of obesity. _Ann. NY Acad. Sci._ **1190**, 1–14 (2010).
18. Tong, T., Shen, Y., Lee, H. W., Yu, R. & Park, T. Adenylyl cyclase 3 haplo-insufficiency confers susceptibility to diet-induced obesity and insulin resistance in mice. _Sci. Rep._ **6**, 34179 (2016).
19. Warrington, N. M. et al. A genome-wide association study of body mass index across early life and childhood. _Int. J. Epidemiol._ **44**, 700–712 (2015).
20. Speliotes, E. K. et al. Association analyses of 249,796 individuals reveal 18 new loci associated with body mass index. _Nat. Genet._ **42**, 937–948 (2010).
21. Wen, W. et al. Meta-analysis identifies common variants associated with body mass index in east Asians. _Nat. Genet._ **44**, 307–311 (2012).
22. Monda, K. L. et al. A meta-analysis identifies new loci associated with body mass index in individuals of African ancestry. _Nat. Genet._ **45**, 690–696 (2013).

23. Stergiakouli, E. et al. Genome-wide association study of height-adjusted BMI in childhood identifies functional variant in *ADCY3*. *Obesity (Silver Spring)* **22**, 2252–2259 (2014).

24. Felix, J. F. et al. Genome-wide association analysis identifies three new susceptibility loci for childhood body mass index. *Hum. Mol. Genet.* **25**, 389–403 (2016).

25. Liu, J. Z. et al. Association analyses identify 38 susceptibility loci for inflammatory bowel disease and highlight shared genetic risk across populations. *Nat. Genet.* **47**, 979–986 (2015).

26. Voisin, S. et al. Many obesity-associated SNPs strongly associate with DNA methylation changes at proximal promoters and enhancers. *Genome Med.* **7**, 103 (2015).

27. Liu, X. et al. Maternal preconception body mass index and offspring cord blood DNA methylation: exploration of early life origins of disease. *Environ. Mol. Mutagen.* **55**, 223–230 (2014).

Author contributions

S.S., A.B., M. Arslan and P.F. designed the study and wrote the first draft of the paper. S.S., Q.M.J., S.M.D., A.H. and M. Arslan collected samples and performed biochemical analyses. A.B., E.D., O.S., T.R., E.V., I.R., S.S. and F.D.G. performed whole-exome sequencing and analyzed the genetic data. J.M., H.A., D.A.S., M. Ali, W.I.K., T.A.B. and C.S. identified and recruited families with obese individuals. F.T., J.G., A.M., G.Q., R.B., A.A. and J.L. performed the functional experiments and analyzed the data. M.U.M. performed the structural analysis. All authors contributed to the final version of the manuscript.

Competing interests

The authors declare no competing financial interests.

Additional information

Supplementary information is available for this paper at https://doi.org/10.1038/s41588-017-0023-6.

Reprints and permissions information is available at www.nature.com/reprints.

Correspondence and requests for materials should be addressed to P.F.

Publisher's note: Springer Nature remains neutral with regard to jurisdictional claims in published maps and institutional affiliations.

Methods

Study subjects. The 138 probands included in this study were part of a larger cohort of 195 subjects with severe obesity (BMI SDS >3). The subjects were recruited from public hospitals in the central province of Punjab, Pakistan, and written consent was obtained from the patients or parents. The study protocol was approved by the ethics and/or research committees of Children's Hospital and the University of Lahore, Lahore, Pakistan. Consent to publish photos was obtained in all cases. Probands and/or their parents were interviewed to obtain family and medical history, and family pedigrees spanning at least three generations were constructed. At initial presentation, the recruitment of the proband and of accompanying parents, if available, was made on a strictly voluntarily basis. In case a homozygous variant suspected of its association with obesity was identified, other members of the affected family were invited to participate in the study, subject to their availability. Clinical cases of syndromic obesity were excluded from the study. Anthropomorphic measurements and physical examination were carried out, and blood samples were obtained in each case for subsequent DNA extraction and biochemical analyses. The single case of a child of European–American ancestry included in the present study was referred to the outpatient clinic in Maastricht University Medical Center to establish the genetic cause of obesity. After receiving genetic counseling the parents provided written consent to participate in the study.

Smell test. Smell testing of probands from Pakistan and their family members was performed at the 'Ear, nose and throat' (ENT) unit of Children's Hospital Lahore. Preceding the test for a possible loss of ability to smell, the subject was thoroughly examined for upper respiratory infections, rhinitis and chronic sinusitis or for the presence of nasal masses such as polyps. A semiquantitative test was administered to assess smell function based on the patient's response to three different sniff odorants, each at four serial dilutions, presented in a random sequence. The subjects were blindfolded before testing. The test was scored (0–12) on the subject's correct responses. The individual scores reflected the extent of loss of olfactory function (normosmia: 10–12; mild to moderate microsmia: 5–9; acute microsmia: 3–4; anosmia: 0–2). No adjustments were made for age or sex. The European–American proband with the compound heterozygous mutation was not tested for smell but was reported to have no sense of smell.

Preliminary genetic screening. All probands (except the European–American case) were primarily screened for pathogenic mutations in the coding exons of *LEP* and *MC4R* by conventional sequencing. A further 27 genes that were known to be associated with nonsyndromic and syndromic obesity were analyzed using a one-step PCR-based microdroplet enrichment step (RainDance Technologies) followed by next-generation sequencing (NGS), as previously described[3] (Fig. 1a). Additionally, genome-wide genotyping was performed to find structural variants in obesity-associated genes. These screening procedures identified 57 probands with homozygous loss-of-function mutations in known obesity-associated genes (published[3–5] and unpublished data).

Whole-exome sequencing (WES) and data analysis. Genomic DNA samples from the remaining 138 probands and their available family members were processed using the Agilent SureSelectXT Human All Exon Kit (version V5 + UTRs; Agilent Technologies) or the NimbleGen SeqCap EZ MedExome Target Enrichment Kit (Roche NimbleGen), following the manufacturer's protocol. The first group of 96 samples processed through the Agilent protocol were sequenced using an Illumina HiSeq 2500 instrument (Illumina) with 100-bp paired-end reads, whereas the second group of 159 samples was processed using the NimbleGen protocol and sequenced using an Illumina HiSeq 4000 instrument (Illumina) with 150-bp paired-end reads. The demultiplexing of sequence data was performed with bcl2fastq2 Conversion Software (Illumina). Subsequently, sequence reads from FASTQ files were mapped to the human genome (hg19/GRC37) using the Burrows–Wheeler Aligner, and a local realignment was processed using the Genome Analysis Toolkit (GATK). Variant calling was performed using GATK HaplotypeCaller. Only genotypes with a sequencing depth of >8× were selected for further analyses. The variant annotation was performed using the Ensembl Perl API and other Perl scripts to include data from the dbSNP and dbNSFP databases. All DNA samples were sequenced with an average read depth of >80×.

For the child of European–American descent, WES analysis was performed in the index patient and both parents (trio approach). Exome capture was carried out using the Agilent SureSelect Human All Exon Enrichment Kit (Agilent Technologies). Sequencing was performed on an Illumina HiSeq platform (BGI, Copenhagen, Denmark), and the data were analyzed with BWA (read alignment) and GATK (variant calling) software packages using default parameters.

Variant prioritization and candidate gene discovery. Autosomal recessive homozygosity for disease-associated mutation(s) was expected in all probands with consanguineous parentage. To identify candidate genes and/or mutations associated with obesity, variations in each family were filtered individually to detect potentially causative homozygous mutations in affected individuals. In the initial filtration step, all heterozygous variants present in obese individuals were removed. Because the likelihood of any novel causative or deleterious variant annotated in publicly available databases is low, variants with an allele frequency of >0.01%

in the 1000 Genomes Project database, the Exome Variant Server (EVS) and the Exome Aggregation Consortium (ExAC) database were excluded. Finally, any homozygous variants in family members exhibiting a normal body weight (BMI <28) were excluded from further analysis. PolyPhen and MutationTaster in silico mutation-prediction software were used to predict pathogenicity. Variants that were synonymous were also removed from further analyses. Potentially deleterious mutations that were present in runs of homozygosity (ROH) were given priority for further analysis. Using this approach (Fig. 1a), an average of ~16,000 high-quality variants were initially identified per individual from paired-end reads, which was reduced to 10–15 variants after filtering (Supplementary Tables 2–4). Genes identified in ≥2 families were considered candidates for obesity. Following these sequential steps, we identified *ADCY3* as a valid candidate gene for obesity.

As a first step, the European–American proband was screened against a diagnostic Kallmann syndrome/hypogonadotrophic hypogonadism (KS/HH) gene panel that included 26 genes associated with KS/HH. No potentially pathogenic 'de novo', homozygous, compound heterozygous or X-linked variants were detected in the coding or splice-site regions of these 26 genes through filtering steps using ESP dbSNP and in-house databases, and dbSNP at a frequency level of <1%. Because of the negative results obtained with the KS/HH panel, we continued by using a stringent filtering regimen for the rest of the variants. This involved filtering for <5% in dbSNP, <1% in the in-house database and >3.5% in phyloP for variants located in coding regions and splice sites. The filtration step reduced the number of variants to 109. One synonymous variant in *ACAD10* was identified based on the GATK score. By filtering for de novo, homozygous or compound heterozygous variants, only three variants were identified (Supplementary Table 7). Of these variants, compound heterozygous variants of *ADCY3* were of most interest, as these corroborated well with the patient's phenotype.

Mutations identified in *ADCY3*. The mutations identified in consanguineous families included a homozygous frameshift mutation c.3315del; p.Ile1106Serfs*3 (*ADCY3*[Mut-I]). This mutation in the last exon (coding exon 21) of the *ADCY3* gene (Fig. 1c and Supplementary Fig. 1) results in a truncated protein by introducing a stop codon after two aberrant amino acids. The second variant, c.2578-1G>A (*ADCY3*[Mut-II]) was identified as a splice-site mutation. Here, the nucleotide substitution abolished the essential splice acceptor site at intron 15 as predicted by the Human Splicing Finder (Supplementary Note). As a result of exon skipping, the mutated protein consists of only 1,091 amino acids instead of the usual 1,144 amino acids. The third homozygous variant, c.191 A>T; p.Asn64Ile (*ADCY3*[Mut-III]) was a missense mutation. The fourth mutation that was identified in a nonconsanguineous European–American family is a compound heterozygous mutation c.1268del; p.Gly423Alafs*19 (*ADCY3*[Mut-IVa]) and c.3354_3356del; p.Phe1118del (*ADCY3*[Mut-IVb]).

Polymerase chain reaction (PCR), sequencing and mutational analysis. Mutations identified in *ADCY3* gene through WES analysis were confirmed in the probands and their family members by standard PCR and Sanger sequencing using a 3730 DNA analyzer (Life Technologies). Sequence traces were analyzed using the Mutation Surveyor software package (SoftGenetics). The PCR primer sequences and thermocycler conditions are available in Supplementary Table 8.

ADCY3 expression analysis. Blood (2 ml) was drawn in PAXgene Blood RNA tubes, and RNA was extracted using the PAXgene RNA Blood kit (Qiagen) according to the manufacturer's instructions. *ADCY3* gene expression was analyzed for P1 (*ADCY3*[Mut-I] homozygote) and a family member (*ADCY3*[Mut-I] heterozygote) by qRT–PCR. Briefly, 300–500 ng of total RNA was converted to cDNA using the High Capacity RNA-to-cDNA Kit (Life Technologies) in a final reaction of 20 μl. Gene expression was performed by TaqMan assay (Life Technologies) using the following primers: hADCY3 FAM (Hs01086502_m1) and internal control housekeeping gene B2M VIC (Hs00984230_m1). All qPCR reactions were set up in triplicate in a 384-well plate (Life Technologies). Each well contained 1 μl of cDNA (diluted 1:3) and 9 μl of the reaction mix, i.e., 5 μl of TaqMan Gene Expression Mix (cat no. 4370048, Life Technologies), 0.5 μl of target and control probes and 3 μl of nuclease-free water to make a total reaction volume of 10 μl. The qPCR was performed using the 7900HT Fast Real-Time PCR System (Life Technologies). The $2^{-\Delta\Delta CT}$ method was used to quantify the level of *ADCY3* in both samples against a standard control.

Whole-genome genotyping. Genome-wide high-density genotyping was performed by using the HumanOmni 2.5 S BeadChip KIT (Illumina) containing >2.5 × 10⁶ variants with a minor allele frequency (MAF) of 2.5%, according to the manufacturer's instructions. A genotyping project was created in GenomeStudio using the standard cluster file, and the genotypes were assigned to each SNP based on the fluorescence intensity data. A reproducibility and heritability report was generated to ensure that the parent-to-child heritability frequency (P-C heritability freq) was ≥0.99. Finally, the cluster file was exported, and reports were generated for subsequent calling of ROH.

Detection of runs of homozygosity (ROH). ROH were detected using the plink open-source whole-genome association analysis toolset to identify an autozygous

region in the affected inbred individuals. The genotyping data were subjected to quality control to remove individuals missing >5% genotype data, excluding SNPs with a MAF ≤0.05, markers that failed to comply with a Hardy–Weinberg threshold of 0.001, and individuals and/or markers on the basis of the Mendelian error rate (ME).

Biochemical determinations. Serum hormone concentrations were measured in duplicate by enzyme-linked immunosorbent assay (ELISA) using commercially available kits (insulin and cortisol, Monobind; leptin, Organium Laboratories), using an EIA analyzer (Bio-Rad Laboratories). Samples were analyzed according to the manufacturer's instructions. The inter-assay and intra-assay variations were <10%. All other biochemical analytes (blood glucose, serum triglycerides, cholesterol, low-density lipoprotein (LDL)-C, high-density lipoprotein (HDL)-C; high-sensitivity C-reactive protein (hsCRP), 25-hydroxy vitamin D, creatinine and blood urea nitrogen) were determined by chemiluminescence assays (CHEMIFLEX). Fasting blood glucose and insulin levels were used to measure homeostasis model assessment of insulin resistance (HOMA-IR).

Molecular modeling. Stepwise molecular modeling was performed to determine the structural consequences of the mutations identified in *ADCY3*. Briefly, homology modeling of hADCY3^{WT} or the ADCY3 mutants was coupled with molecular dynamics (MD) simulations for model refinement. Molecular docking of a magnesium–ATP molecule on the catalytic site followed by a long-run MD simulation of the docked complex was carried out to assess the stability of the backbone of the mutant ADCY3 molecules (Supplementary Figs. 8 and 9). In this study, ADCY3^{Mut-I} (p.Ile1106Serfs*3; the encoded protein has a shorter sequence of 1,108 amino acids, instead of 1,144, after translation of two aberrant amino acids, serine and leucine) and ADCY3^{Mut-II} (c.2578-1 G>A; the encoded protein has a sequence of 1,091 amino acids instead of 1,144) were used for homology modeling with hADCY3^{WT}. In the case of compound heterozygous mutant, ADCY3$^{Mut-IVa}$ and ADCY3$^{Mut-IVb}$ (p.Gly423fs*19 and p.Phe1118del. respectively), the first mutation occurs in the C1 catalytic domain and causes the translation of 18 aberrant amino acids followed by a premature stop codon. Consequently, native folding of this protein is predicted to fail due to a marked truncation of the catalytic domain, and the protein is likely to assume an unpredictable conformation that may lead to a loss of function. PDB IDs 1CS4 for C1 domain and 1AZS to model C2 domain were used. Modeling of the truncated domain conformation was not possible due to a lack of known structural information in the Protein Data Bank (PDB). Further analysis of the hADCY3^{WT} structure showed that the amino acids lacking in p.Gly423fs*19 are normally involved in the interaction with Mg–ATP, the C2 catalytic domain and G$_{αs}$, and correct conformation of this region of the protein is necessary for normal function. Homology models of hADCY3^{WT} and the mutants were refined by MD simulations to further elucidate molecular docking with Mg–ATP. AutoDock Vina[28] was used to study the predicted docked conformations of ADCY3 with ATP and the binding affinity of Mg–ATP at the catalytic interface in hADCY3^{WT} and the mutant ADCY3 proteins. Assessment of ATP–Mg docking at the interface of both ADCY3 catalytic domains, where cAMP is catalyzed in response to G protein signaling, was performed as described (Supplementary Note). To further investigate the stability of docked complexes, a production-simulations run of 200 ns at 300 K and 1 bar pressure in explicit solvation model (with TIP3P water module) was performed in each case after a stepwise minimization and equilibration. The AMBER 16 simulation package was used throughout for all simulations (see Supplementary Note for detailed protocol).

Generation of constructs expressing wild-type or mutant ADCY3. Full-length *ADCY3* was amplified from a human *ADCY3* cDNA clone (NM_004036, cat. no. RC220272; Origene, Maryland, USA) using Q5 High-Fidelity DNA Polymerase (New England BioLabs, Massachusetts, USA). The forward and reverse primers, showing restriction sites for AscI and NotI, respectively, are given in Supplementary Table 9. The resulting 3.4-kb PCR fragment was verified by gel electrophoresis, digested with AscI and NotI, and column-purified. The AscI–NotI fragment with the *ADCY3* gene was then cloned into the polylinker of the pCMV6-AN-Myc mammalian expression vector, which contains an N-terminal Myc tag (Origene, cat. no. PS100012). The ligated plasmid was transformed in DH5α competent cells (Invitrogen, California, USA), which were then plated onto ampicillin-containing (50 μg/ml) LB agar (Sigma) medium, and individual colonies were analyzed after 24 h of growth at 37 °C. The resulting wild-type plasmid (Myc-hADCY3^{WT}) was verified by sequencing. Each of the four *ADCY3* mutations (*ADCY3^{Mut-I}*, *ADCY3^{Mut-II}*, *ADCY3$^{Mut-III}$* and *ADCY3$^{Mut-IVb}$*) was introduced into the Myc-hADCY3^{WT} plasmid by site-directed mutagenesis using the Q5 Site-Direct Mutagenesis kit (New England BioLabs). Primers for mutagenesis were designed according to the manufacturer's recommendations, and the sequences (5′ to 3′) are given in Supplementary Table 10. The amplified products were transformed into DH5α cells as described above, and the plasmid sequences were again verified by sequencing before functional analyses. pcDNA3 without any inserted DNA sequence was used as the control plasmid in cell-based assays.

Cell culture and transient transfection. Chinese hamster ovary (CHO) cells (ATCC) were maintained in a volume ratio of 1:1 Dulbecco's modified

Eagle's medium with nutrient mixture F12 (DMEM/F12) (Thermo Fisher Scientific) supplemented with 10% fetal calf serum (FCS) and 1% penicillin–streptomycin mixture (Sigma-Aldrich). Baby hamster kidney (BHK) cells (ATCC) were maintained in BHK medium (DMEM, 10% FCS, 10 mM HEPES, 2 mM glutamine) in a humidified incubator at 37 °C with 5% CO$_2$. Cells were passaged by trypsinization every 3 d. A total of 3,000 BHK cells/well were seeded in 24-well plates (Nalge Nunc International) with or without 18-mm-in-diameter glass cover slips and cultured in BHK medium. After 72 h, cells were transfected with 500 ng of the indicated plasmids using 0.5 μl jetPEI (Polyplus, Illkirchen, France) in 1.1 ml BHK medium. After 72 h, the wells were washed with PBS before further analysis.

Protein blotting. For protein blotting, cells were detached in PBS containing 10 mM EDTA at 37 °C and concentrated by centrifugation, and the pellets were resuspended in Laemmli's sample buffer followed by brief sonication. Samples were separated by SDS-PAGE (10% gel), and subsequent immunoblotting was performed using rabbit anti-Myc antibodies (1:3,000; Sigma, C3956) or anti-ADCY3 (raised against the extracellular domain; 1:1,000; Alomone Labs, Jerusalem, Israel) as previously described[29]. Secondary antibodies (horseradish peroxidase (HRP)-coupled donkey anti-rabbit; GE Healthcare) were used at a 1:3,000 dilution, and binding was detected by ECL (GE Healthcare). Proteins were detected by Ponceau's stain, and all blots were imaged using FLUORCHEM 8000 (Alpha Innochem).

Immunocytochemistry. Cells grown on coverslips were washed in PBS, fixed with 4% paraformaldehyde in PBS, permeabilized with 2% saponin and incubated with antibodies, as previously described[29]. The antibodies, rabbit anti-Myc (1:300; Sigma, C3956) and anti-ADCY3 (Alomone Labs), were used at a dilution of 1:100. The secondary antibodies were used at a 1:3,000 dilution (Cy3 donkey anti-rabbit, Jackson ImmunoResearch). Confocal analysis was performed as previously described[29] using a Zeiss LSM 510 meta-confocal microscope (Zeiss, Göttingen, Germany) with an ApoPLAN 63× objective lens.

cAMP assay. Levels of cAMP production were determined at 37 °C in BHK cells that had been transfected with pcDNA3 or with plasmids expressing Myc-tagged hADCY3^{WT} or the mutants. Cells were washed in Krebs–Ringer buffer (KRB) (135 mM NaCl, 3.6 mM KCl, 5 mM NaHCO$_3$, 0.5 mM NaH$_2$PO$_4$, 0.5 mM MgCl$_2$, 10 mM HEPES, 1.5 mM CaCl$_2$, 5 mM glucose, 0.1% BSA; pH 7.4) and subsequently incubated for 30 min in KRB in the presence or absence of 2 μM forskolin and 0.1 mM IBMX[30]. Following incubation, KRB was aspirated, and the cells were solubilized with a solution of 0.1 M HCl and 1% Triton X-100 (300 μl/well) at 37 °C for 30 min. The cell solution was centrifuged at 600 g for 5 min at 4 °C, and the supernatants were either stored at –80 °C or assayed directly using the Cyclic AMP Direct EIA Kit (Arbor Assays). Total protein content of the supernatants was determined by the bicinchoninic acid (BCA) assay (Thermo Fisher Scientific).

Luciferase activity. CHO cells (1 × 10^5) were plated in 96-well dishes and transiently transfected with 1 μg of plasmid, which included 400 ng of CreLuc reporter[31] with 50 ng pCMV-betaGal (for normalization) plus 100 ng of the ADCY3 expression plasmids or the empty vector, using the FuGENE 6 transfection reagent (Promega) according to the manufacturer's protocol. After transfection (44 h) the cells were incubated with fresh medium supplemented with 2% FCS and 100 μM IBMX plus 1 μM forskolin or DMSO (vehicle) for 4 h. The cells were then washed with PBS and lysed using Passive Lysis Buffer (Promega). O-nitrophenyl-β-D-galactopyranoside (ONPG) was used as the substrate for β-galactosidase activity, and the colored reaction product was measured with a microplate reader at an absorbance wavelength of 450 nm. Luciferase activities were measured with 25 μl of the protein extract by using the Luciferase Reporter Assay system (Promega) according to the manufacturer's protocol. Luciferase activity was calculated as relative luminescence units (RLUs) normalized against β-galactosidase activity.

Statistical analysis. Statistical analysis was carried out using OriginPro 8.5.0. Significance of differences was calculated by performing unpaired one-way ANOVA and a Bonferroni post hoc test. The number of times an experiment was performed and the number of replicates in each case are provided in figure legends (Fig. 2d and Supplementary Figs. 3b, 6 and 7). Actual *P* values (considered up to three decimal places) are given in the relevant figure legends. Wherever necessary, single data points of independent experiments are also represented.

URLs. ExAC browser, http://exac.broadinstitute.org/; UCSC Genome Browser, http://genome.ucsc.edu/; PolyPhen-2, http://genetics.bwh.harvard.edu/pph2/index.shtml; Exome Variant Server, http://evs.gs.washington.edu/EVS/; Human splicing finder, http://www.umd.be/HSF/; Plink, http://zzz.bwh.harvard.edu/plink/download.shtml; SoftGenetics, http://www.softgenetics.com/mutationSurveyor.php; GATK, https://software.broadinstitute.org/gatk/documentation/tooldocs/current/org_broadinstitute_gatk_tools_walkers_haplotypecaller_HaplotypeCaller.php.

Life Sciences Reporting Summary. Further information on experimental design is available in the Life Sciences Reporting Summary.

Data availability. The sequencing data (FASTQ files) of the probands with *ADCY3* mutation included in this study have been deposited in the NCBI Sequence Read Archive database under accession numbers SAMN07490276 (F1, mut I), SAMN07490319 (F2, mut II) and SAMN07490318 (F3, mut III).

References

28. Trott, O. & Olson, A. J. AutoDock Vina: improving the speed and accuracy of docking with a new scoring function, efficient optimization and multithreading. *J. Comput. Chem.* **31**, 455–461 (2010).
29. Boal, F., Laguerre, M., Milochau, A., Lang, J. & Scotti, P. A. A charged prominence in the linker domain of the cysteine-string protein Cspα mediates its regulated interaction with the calcium sensor synaptotagmin 9 during exocytosis. *FASEB J.* **25**, 132–143 (2011).
30. Roger, B. et al. Adenylyl cyclase 8 is central to glucagon-like peptide 1 signaling and effects of chronically elevated glucose in rat and human pancreatic beta cells. *Diabetologia* **54**, 390–402 (2011).
31. Ferdaoussi, M. et al. Exendin-4 protects beta cells from interleukin-1β -induced apoptosis by interfering with the c-Jun NH$_2$-terminal kinase pathway. *Diabetes* **57**, 1205–1215 (2008).

nature research

Corresponding author(s): Philippe Froguel

☐ Initial submission   ☒ Revised version   ☐ Final submission

Life Sciences Reporting Summary

Nature Research wishes to improve the reproducibility of the work that we publish. This form is intended for publication with all accepted life science papers and provides structure for consistency and transparency in reporting. Every life science submission will use this form; some list items might not apply to an individual manuscript, but all fields must be completed for clarity.

For further information on the points included in this form, see Reporting Life Sciences Research. For further information on Nature Research policies, including our data availability policy, see Authors & Referees and the Editorial Policy Checklist.

▶ Experimental design

1. Sample size

Describe how sample size was determined.

The probands with severe early onset obesity were recruited on presentation at the paediatric units of hospitals situated in the Punjab province of Pakistan. The objective was to identify cases of monogenic obesity. The family members when available, were also recruited in the study. The nature of study did not allow sample size calculatation, a priori.

2. Data exclusions

Describe any data exclusions.

Obese subjects with clinical syndromic obesity were not recruited.

3. Replication

Describe whether the experimental findings were reliably reproduced.

All experimental observations/findings were successfully replicated rand the results reliably reproduced.

4. Randomization

Describe how samples/organisms/participants were allocated into experimental groups.

Grouping of samples/patients was not applicable to this study.

5. Blinding

Describe whether the investigators were blinded to group allocation during data collection and/or analysis.

Not blinded

Note: all studies involving animals and/or human research participants must disclose whether blinding and randomization were used.

6. Statistical parameters

For all figures and tables that use statistical methods, confirm that the following items are present in relevant figure legends (or in the Methods section if additional space is needed).

n/a	Confirmed	
☐	☒	The exact sample size (n) for each experimental group/condition, given as a discrete number and unit of measurement (animals, litters, cultures, etc.)
☐	☒	A description of how samples were collected, noting whether measurements were taken from distinct samples or whether the same sample was measured repeatedly
☐	☒	A statement indicating how many times each experiment was replicated
☐	☒	The statistical test(s) used and whether they are one- or two-sided (note: only common tests should be described solely by name; more complex techniques should be described in the Methods section)
☒	☐	A description of any assumptions or corrections, such as an adjustment for multiple comparisons
☐	☒	The test results (e.g. P values) given as exact values whenever possible and with confidence intervals noted
☐	☒	A clear description of statistics including central tendency (e.g. median, mean) and variation (e.g. standard deviation, interquartile range)
☐	☒	Clearly defined error bars

See the web collection on statistics for biologists for further resources and guidance.

► Software

Policy information about availability of computer code

7. Software

Describe the software used to analyze the data in this study.

> Burrows-Wheeler Aligner ; GATK; MutationTaster; Polyphen-2;; bcl2fastq2 Conversion Software (Illumina); Mutation Surveyor package (SoftGenetics), AMBER 16 simulation package and PLINK version 1.7.

For manuscripts utilizing custom algorithms or software that are central to the paper but not yet described in the published literature, software must be made available to editors and reviewers upon request. We strongly encourage code deposition in a community repository (e.g. GitHub). *Nature Methods* guidance for providing algorithms and software for publication provides further information on this topic.

► Materials and reagents

Policy information about availability of materials

8. Materials availability

Indicate whether there are restrictions on availability of unique materials or if these materials are only available for distribution by a for-profit company.

> Not applicable

9. Antibodies

Describe the antibodies used and how they were validated for use in the system under study (i.e. assay and species).

> For Immunofluorescence and Western blotting: Rabbit anti-Myc (Sigma) and Rabbit anti-ADCY3 (Alomone). Immunoassay of hormones was performed using commercially available ELISA kits

10. Eukaryotic cell lines

a. State the source of each eukaryotic cell line used.

> The CHO and BHK cells were obtained from ATCC

b. Describe the method of cell line authentication used.

> No authentication used

c. Report whether the cell lines were tested for mycoplasma contamination.

> No

d. If any of the cell lines used are listed in the database of commonly misidentified cell lines maintained by ICLAC, provide a scientific rationale for their use.

> No

► Animals and human research participants

Policy information about studies involving animals; when reporting animal research, follow the ARRIVE guidelines

11. Description of research animals

Provide details on animals and/or animal-derived materials used in the study.

> Not applicable

Policy information about studies involving human research participants

12. Description of human research participants

Describe the covariate-relevant population characteristics of the human research participants.

> The study is based on WES analysis in 138 probands with early onset severe non syndromic obesity with a BMI SDS of >3.0, that were found negative for mutations in known obesity associated genes. Family members subject to their availability, were also recruited (n= 117).   The probands were recruited on presentation at the paediatric units of hospitals situated in the Punjab province of Pakistan. Written consent was obtained in all cases.